Clay Minerals, (2017) **52**, 427–438

High-performance PTFE nanocomposites based on halloysite nanotubes

ZHI-LIN CHENG[1,*], XING-YU CHANG[1], ZAN LIU[1], DUN-ZHONG QIN[1,3] AND AI-PING ZHU[1,2]

[1] *School of Chemistry and Chemical Engineering, Yangzhou University, Yangzhou 225002, China*
[2] *Zhenjiang High Technology Research Institute of Yangzhou University, Zhenjiang 212000, China*
[3] *Jiangsu Sinvochem Co. Ltd., Yangzhou 225002, China*

(*Received 30 August 2017; revised 22 November 2017; Guest Associate Editor: Pilar Aranda*)

ABSTRACT: Halloysite nanotubes (HNTs)/polytetrafluoroethylene (PTFE) nanocomposites were prepared by the cold compression moulding method. The effects of addition of HNTs (HNTs 'filling') on the performances of PTFE were explored using X-ray diffraction, Fourier Transform infrared spectroscopy, scanning electron microscopy and thermogravimetric analysis which showed that HNTs were well dispersed in the PTFE matrix by means of physical mixing at lower contents of 2–5 wt.%; the introduction of HNTs into PTFE could improve the heat stability of the PTFE. Furthermore, the mechanical and tribological performances of the nanocomposites were measured to examine the filling effect. The tensile strength of the HNTs/PTFE nanocomposites at 2–5 wt.% HNTs content increased by ~3.5% while their wear rates decreased by 55–90% relative to pure PTFE, clear proof of the filling effect of HNTs with a high aspect ratio.

KEYWORDS: PTFE, HNTs, nanocomposites, mechanical, tribological.

Polytetrafluoroethylene (PTFE) is a common material. Due to the superior thermal stability, chemical resistance and lower friction coefficient of PTFE, it is found in many fields: *e.g.* aerospace, chemical, medical, automotive and electronics. Its poor wear behaviour, however, limits the applications in wear resistance. In recent decades, fillers, especially nanomaterials, have been added to the PTFE to investigate possible improvements to the wear resistance.

The filling method has been demonstrated to be the most effective and convenient way of improving the wear resistance. Recent use of micro- or nano-scale particles as fillers has been studied extensively to improve the thermal stability, hardness and wear behaviour of the PTFE composites.

* E-mail: zlcheng224@126.com
https://doi.org/10.1180/claymin.2017.052.4.02

Polymer composites reinforced by microscale fibres have been used widely in high-technology industries for many years because of their outstanding mechanical and tribological properties. In a study of carbon fibre/PTFE composites, Liu *et al*. (2012) reported that the composites filled with 50 vol.% filler content showed the lowest friction coefficient (0.15), which was 24.6% less than pure PTFE while the wear rate fell by a factor of 100 times compared to the pure PTFE. Vohra *et al*. (2016) reported that the wear loss of the glass fibre/PTFE composites decreased substantially with increase in the glass fibre content and the minimum wear loss was at 25% for glass-filled PTFE. Klaas *et al.* (2005) studied three forms of glass:. glass fibres, glass beads and glass flakes, each with a content of 25 wt.% filled PTFE, finding that the glass fibres showed least wear.

Nanoscale materials have attracted much interest because of the unique characteristics of nanoparticles, including large surface area, surface reactivity and

dramatic improvement in the wear behaviour of the composites. Vail *et al*. (2009) reported that the wear resistance of the single-walled carbon nanotube (CNT)-filled PTFE composite with 2 wt.% filler content improved by >20 times and the friction coefficient increased by ∼50%. McElwain *et al*. (2008) studied the PTFE composites filled with nanoscale alumina particles. When the addition of alumina nanoparticles was at 5 wt.%, the wear rate was reduced drastically to ∼10–7 mm^3/Nm, 1000 times less than that of pure PTFE. Krick *et al*. (2015) reported that the nanostructured alumina microfiller-filled PTFE exhibited an extraordinary wear resistance at a small filling amount of alumina (<5 wt.%) and the wear rate of the PTFE composites reduced by more than four orders of magnitude. Chen *et al*. (2003) studied the tribological behaviour of CNTs-filled PTFE composites and the results showed that the wear rate of the CNTs/PTFE composite with 20 vol.% CNT filling was only 1/290 that of pure PTFE. Lee *et al*. (2007) reported the wear and frictional properties of PTFE nanocomposites reinforced with carbon nanoparticles. The wear resistance of PTFE nanocomposites was found to be enhanced by the addition of 2 wt.% of carbon nanoparticles and the wear coefficient of PTFE film decreased from 16.2 to 3.5×10^{-6} mm^3/Nm by the addition of carbon-based nanoparticles heat-treated at 1000°C.

Halloysite nanotubes are naturally occurring aluminosilicates ($Al_2(OH)_4Si_2O_5{\cdot}nH_2O$) with nanotubular structures. The HNTs are found widely in soils in wet tropical and subtropical regions, in weathered rocks and in soils generated from volcanic ash and are available in abundance in China, Japan, France, Brazil, Belgium, Australia and New Zealand. Due to the nanotubular shape of HNTs, they possess highly meso/macroscopic pore structure and large specific surface area. The HNTs range in length from 0.2 to 2 μm. The inner and out diameters range 10–40 nm and 40–70 nm, respectively. Most of the hydroxyaluminium groups (Al-OH) are located in the interior of the HNTs, while the outer portions of the HNTs contain primary siloxanes and a few silanol/aluminol groups that are exposed in the edges of the sheets. HNTs as fillers have exhibited many promising applications in polymers due to their inherent hollow nanotube structure and different outer and inner chemistry (Liu *et al.*, 2007a,b, 2013a,b, 2016a,b; Lvov & Abdullayev, 2013). Compared to CNTs, HNTs also have the advantages of high stability, resistance to organic solvents and ease of disposal or reusability. The HNTs have been shown to be an ideal reinforcement agent for fabricating polymeric composites with improved mechanical performance (Ismail *et al*., 2008; Pasbakhsh *et al*., 2009; Jia *et al*., 2009).

Many HNTs-filled polymer nanocomposites used as fillers have been discovered in recent years. Liu et al (2007a,b) studied HNTs co-cured with epoxy/cyanate ester resin to form organic-inorganic hybrids and found that the moduli of the hybrids in the glassy state and rubbery state were significantly greater than those for the plain cured resin. They also developed HNTs compounded with polylactide (PLA) *via* melt mixing which formed biodegradable and biocompatible clay polymer nanocomposites (CPN) (Liu *et al*., 2013a). Their results showed that the modulus, strength and toughness of the HNTs-PLA nanocomposites were substantially greater than those of unmodified PLA. The study reported by Handge *et al*. (2010) showed that HNTs were promising and inexpensive candidates for improving the stiffness of PA6 while retaining other properties. The study of Čermák *et al*. (2016) showed a certain increment in the tensile modulus from 99.57 MPa (pure LLDPE) to 121.41 MPa (LLDPE filled with 7 wt.% HNTs), an increase of ∼21% compared to pure LLDPE. The report by Carli *et al*. (2014) indicated that the toughness, strain at break and impact strength of the polyhydroxybutyrate valerate copolyester (PHBV) nanocomposites filled with HNTs modified with several silane coupling agents with 3 wt.% HNTs were increased by ∼4, 3 and 1.10 times, respectively. Ye *et al*. (2011) reported that both the storage modulus and Tg of the HNT-toughened epoxy/carbon fibre composites were slightly improved with the addition of HNTs and the Izod impact strength was enhanced by as much as 25% at a 2 wt.% HNTs content. Dong *et al*. (2015) reported that the tensile modulus and strength of the fabricated PLA/HNTs nanocomposite were increased by 3 and 1.34 times at 10 wt.% and 1 wt.% HNTs contents, respectively.

Here, the PTFE nanocomposites filled with different amounts of HNTs were prepared by the cold compression moulding method. The structure and properties of the HNTs/PTFE nanocomposites were determined using a range of techniques. The mechanical properties and tribological behaviours of the nanocomposites were also studied.

EXPERIMENTAL PROCEDURES

Materials and methods

The HNTs were purchased from Yangzhou Xigema New material Co. Ltd. They were purified before use

https://doi.org/10.1180/claymin.2017.052.4.02 Published online by Cambridge University Press

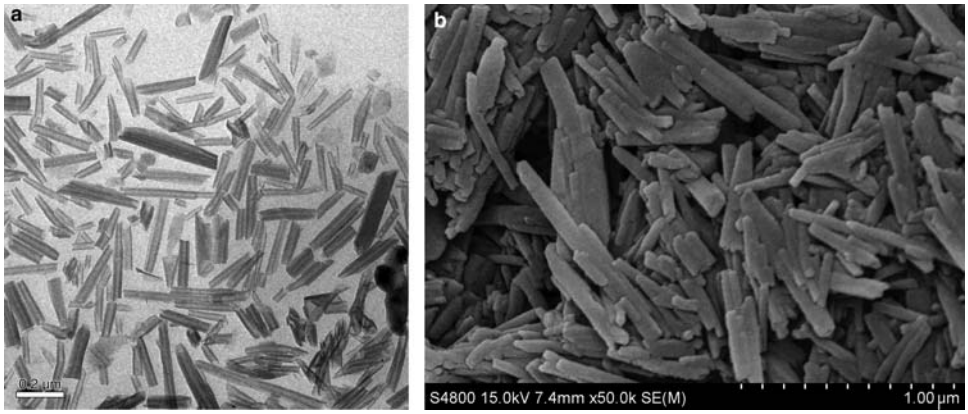

FIG. 1. The morphology of the acid-washed HNTs: (a) TEM; (b) SEM.

by repeated acid-washing (Cheng & Sun, 2016). An amount of HNTs powder was dispersed in 0.5 wt.% HCl aqueous solution under vigorous stirring at 60°C for 6 h, followed by centrifugation and acid-washing at least three times. Finally, the purified product was dried at 60°C in the oven for further use. The morphology of the purified HNTs with few impurities was illustrated in Fig. 1. The chemical composition of the acid-treated HNTs is: SiO_2 (54.51 wt.%), Al_2O_3 (28.84 wt.%), Fe_2O_3 (2.96 wt.%), CaO (4.25 wt.%), MgO (0.21%), Na_2O (1.45 wt.%), K_2O (2.89 wt.%), TiO_2 (1.39 wt.%), ZnO (0.22 wt.%), ZrO_2 (0.45 wt.%), SO_3 (0.65 wt.%) and other (2.18 wt.%).

The PTFE (purchased from Shanghai 3F New Material Co. Ltd.) and HNTs were mixed mechanically using a high-speed (3000 rpm) stirrer for 2 h. The specimens were prepared by compression moulding at a pressure of 10 MPa at room temperature. The specimens were then sintered at 375°C and held for 2 h. Finally, the samples were cooled to room temperature. The mass fraction of HNTs in the nanocomposite ranged from 0 to 20 wt.%, as listed in Table 1.

TABLE 1. The composition of PTFE nanocomposites.

Material	PTFE (wt.%)	HNT (wt.%)
PTFE	100	0
PTFE-1	98	2
PTFE-2	95	5
PTFE-3	90	10
PTFE-4	85	15
PTFE-5	80	20

Mechanical performance testing

The tensile testing was carried out using a WDW-5 instrument (Shanghai Longhua, China). The tensile speed was 50 mm/min. The sample size was 42.8 mm × 5.9 mm × 0.8 mm. Each specimen was tested five times to acquire the mean value. The thickness of each specimen was the average of five measurements taken along the gauge length with a digital micrometer. All the data were shown as a mean ± standard deviation. A one-way analysis of variance (ANOVA) was performed to compare the mean values among different groups.

Tribological-property testing

Tribological testing was performed using a MMW-1 instrument (Jinan Chenda Ltd. Co., China), a ring-on-ring friction and wear tester. The contact schematic diagram of frictional parts is shown in Fig. 2.

The test parameters and environmental conditions were as follows:

Applied load: 200 N
Rotating speed: 200 rpm
Test duration: 60 min
Temperature: 25 ± 2°C
Relative humidity: 50 ± 10%

The friction coefficient was obtained automatically. The wear rate, K (cm^3/h) was calculated according to the following equation:

$$K = \frac{dv}{dT} \quad (1)$$

$$V = \frac{\Delta m}{\rho} \quad (2)$$

https://doi.org/10.1180/claymin.2017.052.4.02 Published online by Cambridge University Press

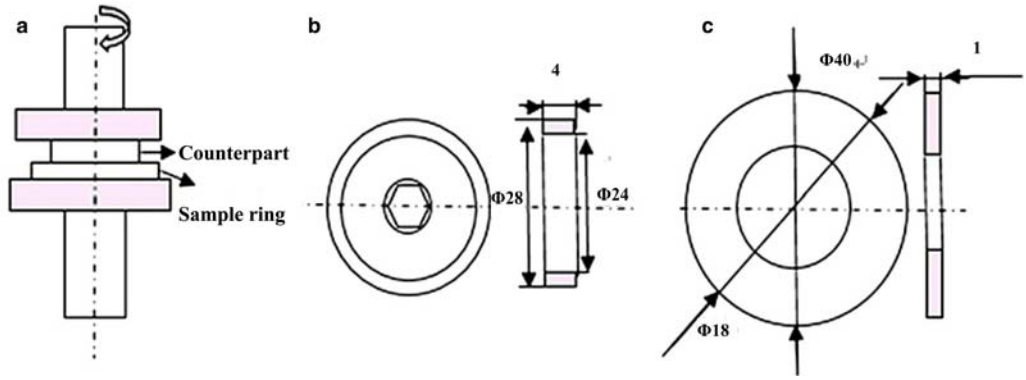

FIG. 2. Schematic diagram of wear tester: (a) ring-on-ring contact; (b) counterpart ring; and (c) sample ring.

where dV and dt were the volume loss and the sliding time, respectively; Δm was the mass loss (mg) and ρ was the density of PTFE composites (g/cm^3).

Characterization

X-ray diffraction (XRD) analysis was performed using a Bruker D8 Advance instrument (Germany) (Cu-$K\alpha$ radiation; background noise: <0.4 CPS; voltage: 40 kV; current: 40 mA; scanning speed: 0.1°2θ; scanning range: ~5–70°2θ. The Fourier transform infrared spectra were recorded on a Cary 610/670 micro IR spectrometer with a resolution of 4 cm^{-1} over the range 4000–400 cm^{-1} using KBr wafers containing 0.5% of sample in single reflection ATR attachment (Varian, USA). Scanning electron microscopy (SEM) images were recorded using an Hitachi S-4800 SEM (Japan) at an acceleration voltage of 10 keV on gold-coated samples. Thermogravimetric Analysis (TGA) was performed using a Perkin Elmer (USA) Pyris 1 analyser at a heating rate of 5°C/min in a nitrogen atmosphere. The wear-scar images were captured using an LSM 700 3D laser scanning microscope (CARL ZEISS, Germany).

RESULTS AND DISCUSSION

Characterization of PTFE filled with different amounts of HNTs

Figure 3a shows the XRD patterns of the as-received HNTs, pure PTFE and HNTs/PTFE nanocomposites. The as-received HNTs show three diffraction maxima at 7.3, 4.5 and 3.6 Å, corresponding to the (001), (020) and (002) reflections (Pasbakhsh *et al*., 2010; Dong *et al*., 2015). The lack of a 10 Å maximum suggests that the as-received HNTs used are fully dehydrated, *i.e.* 7 Å-HNTs (Liu *et al*., 2013a,b,c; Dong *et al*.,

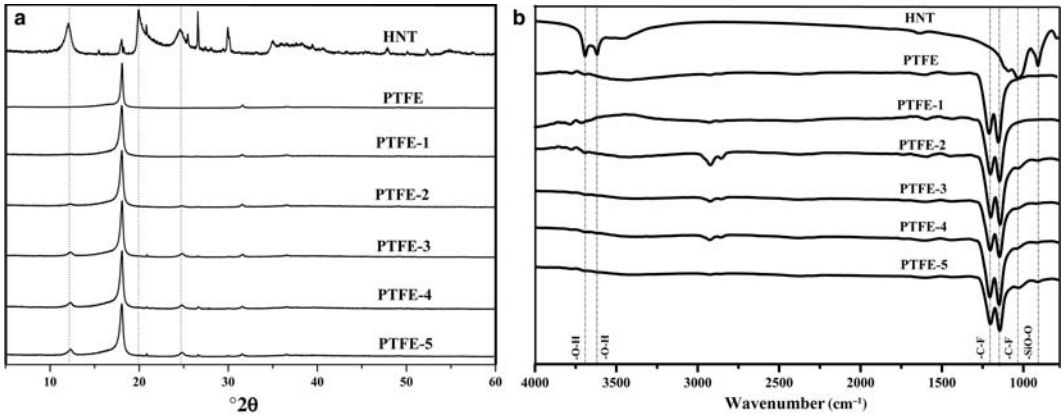

FIG. 3. XRD patterns and FTIR spectra of as-received HNTs, pure PTFE and HNTs/PTFE nanocomposites.

https://doi.org/10.1180/claymin.2017.052.4.02 Published online by Cambridge University Press

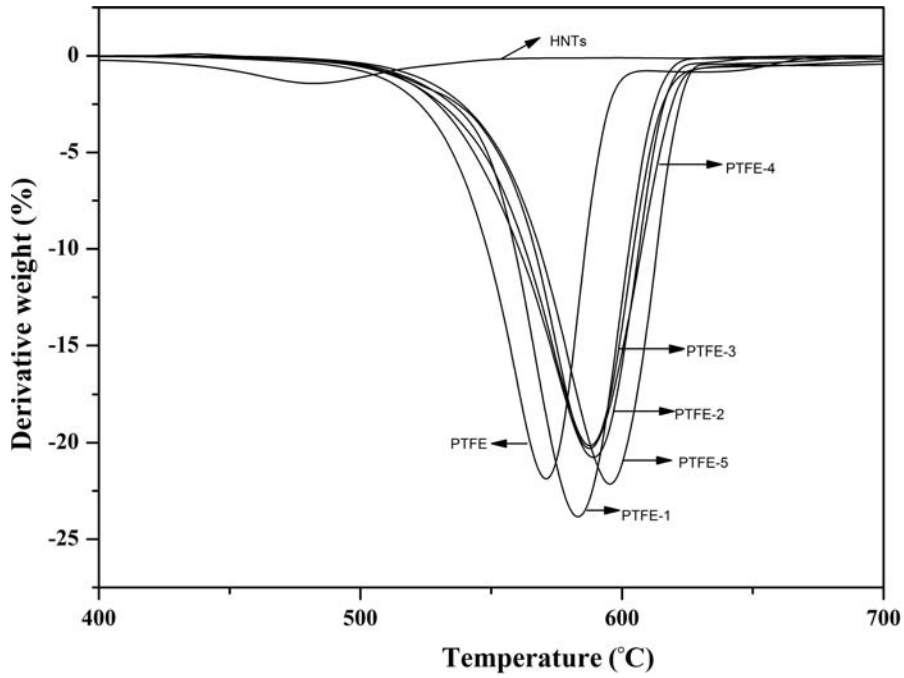

FIG. 4. TG curves of PTFE and HNT/PTFE nanocomposites: HNTs, PTFE, PTFE-1, PTFE-2, PTFE-3, PTFE-4 and PTFE-5.

2015). As for the HNTs/PTFE nanocomposites, the typical peaks above appear gradually with increase in the HNTs contents in the PTFE nanocomposites. The (020) peak of HNTs disappeared in the nanocomposites because the HNTs have a uniform orientation in the HNTs/PTFE nanocomposites. The orientation is a result of the shear force during processing and suggests that interfacial interactions occur between the PTFE and the HNTs. The orientation of HNTs can improve the mechanical and thermal properties of the polymer (Liu *et al*., 2014). The typical peaks for pure PTFE and for HNTs/PTFE nanocomposites located at 18.1°2θ are strong and sharp, indicating that both the pure PTFE and HNTs/PTFE nanocomposites have high proportions of crystalline structures. The addition of HNTs does not alter the crystalline structures of the PTFE.

The FTIR spectra of HNTs, pure PTFE and HNTs/PTFE nanocomposites are shown in Fig. 3b. The as-received HNTs have two intense bands at 3621 and 3694 cm^{-1} which represent AlAlOH stretching. The bands at 1033 and 910 cm^{-1} are associated with stretching of Si-O and Al-OH groups, respectively (Liu *et al.*, 2014). With respect to pure PTFE, the intense absorption bands at 1145 and 1201 cm^{-1} are associated with C–F stretching vibrations, characteristic absorption bands for PTFE (Kwong *et al*., 2006). In the HNTs/PTFE nanocomposites, the intense bands at 3621 cm^{-1} and 3694 cm^{-1} disappear. This might be because of either the destruction of the OH groups at the surface of HNTs by sintering or due to to the dilution of the HNTs contents in the PTFE matrix. The intensity of the HNTs bands at 1033 and 910 cm^{-1} in the PTFE/HNTs nanocomposites is less than those of pure HNTs due to the small mass fraction of HNTs in nanocomposites. These results suggest that HNTs were incorporated successfully into the PTFE matrix.

Figure 4 displays the TGA curves of as-received HNT, of pure PTFE and of HNTs/PTFE nanocomposites. The main weight loss of HNTs due to dehydroxylation occurs at ~488°C. The weight loss of pure PTFE takes place at ~500°C. The weight loss of nanocomposites of PTFE filled with 1–2 wt.% HNTs is in range 2–15 wt.% and occurs at a slightly higher temperature than the pure PTFE. The best thermal stability for polymer clay nanocomposites was observed for larger amounts of HNTs, due to the good heat resistance of HNTs, in agreement with previous studies (Lim *et al*., 2002; Ahmadi *et al*., 2005; Leszczyńska *et al*., 2007). The special structure of HNTs protects the

https://doi.org/10.1180/claymin.2017.052.4.02 Published online by Cambridge University Press

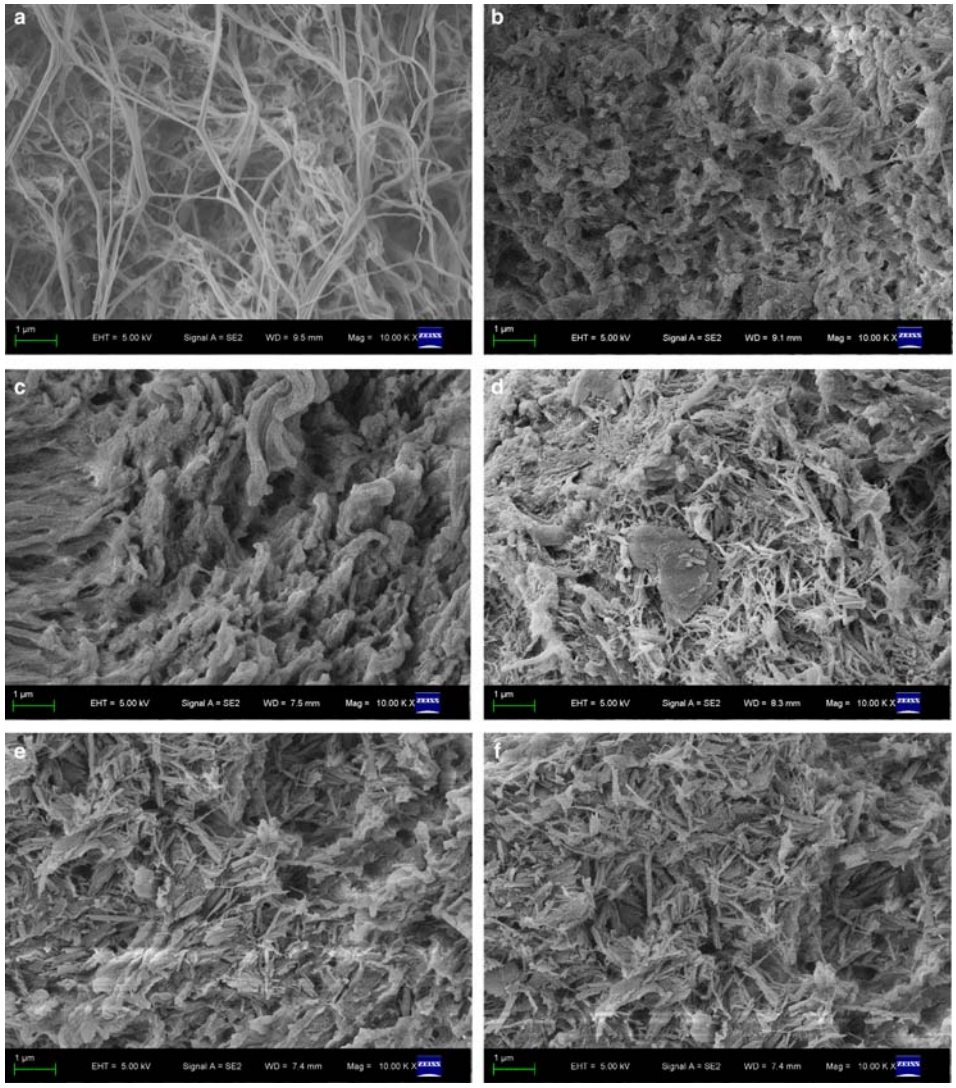

FIG. 5. SEM images of broken surfaces of PTFE and HNT/PTFE nanocomposites: (a) PTFE; (b) PTFE-1; (c) PTFE-2; (d) PTFE-3; (e) PTFE-4; and (f) PTFE-5. Scale bars: 1 μm.

polymer by slowing the escape of volatile products during degradation. These results indicate that HNTs enhance the thermal stability of PTFE (Du *et al*., 2006).

Micrographs of broken surfaces of the pure PTFE and HNTs/PTFE nanocomposite illustrating the dispersion of HNTs are shown in Fig. 5. The pure PTFE contains many ductile microfibrils and drawn ligaments (Fig. 5a). Fracturing of PTFE generates a large volume of intense fibrillation and ductile tears indicating that it consumes much energy. This is in accordance with the high tensile strength of pure PTFE. The HNTs/PTFE nanocomposites have a porous structure with a few extended HNTs (Fig. 5b,c). Some HNTs are separated from the PTFE matrix during fracturing, but otherwise, the dispersion of HNTs was good, probably because the concentration of HNTs was low. The aggregation level of the HNTs increased significantly with increase in the concentration of HNTs (Fig. 5d–f). In addition there is poor adhesion between the HNTs and the PTFE matrix. This is the reason for the decrease in the tensile stress of the nanocomposites with a high proportion of HNTs.

https://doi.org/10.1180/claymin.2017.052.4.02 Published online by Cambridge University Press

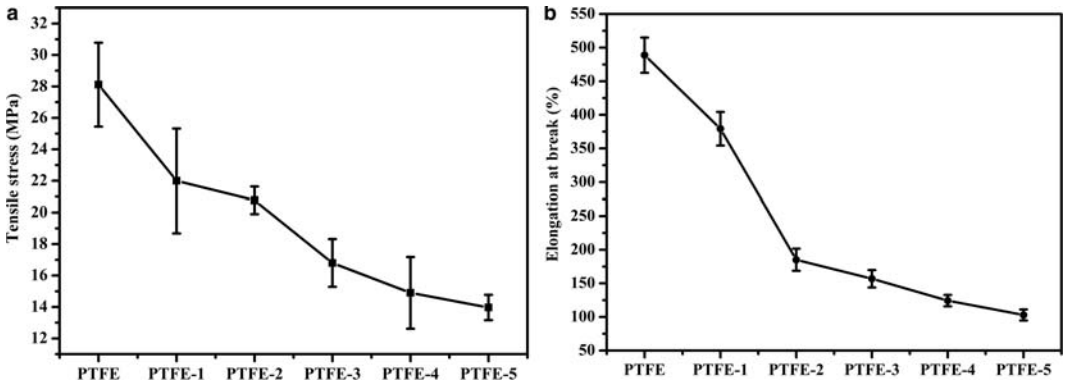

FIG. 6. Tensile strength and elongation at break of PTFE and PTFE/HNT nanocomposites.

Mechanical and friction performance of HNTs/PTFE nanocomposites

Figure 6 shows the tensile strength and elongation at break of pure PTFE and HNTs/PTFE nanocomposites. The nanocomposites with 2 wt.% HNTs show an increase in tensile strength compared with that of pure PTFE (Figure 6a). At low HNTs content, the HNTs can be dispersed uniformly in the matrix leading to the increase in tensile strength. The uniform filler dispersion is important in terms of allowing the matrix to distribute the force to the fillers which carry most of the applied load and which are thus able to stand the stress (Razi *et al*., 2003). However, as the mass fraction of HNTs is increased, the tensile strength of the nanocomposites drops. This is due to stronger filler–filler interaction than filler–resin interaction which is responsible for lower tensile strength as obtained at a greater proportion of HNTs (Ahmadi *et al*., 2005). As can been seen in Fig. 6b, the elongation at break of the HNTs/PTFE nanocomposites reduces with successive additions of HNTs to the polymer. Addition of further HNTs to the PTFE matrix increases the stiffness of the resulting nanocomposites which leads to a reduction in the value of elongation at break.

Figure 7 shows the variation of friction coefficient and volume loss of pure PTFE and HNTs/PTFE nanocomposites. The friction coefficients of the nanocomposites are in the range 0.14–0.23; they change rapidly at the beginning and then maintain a constant value due to the formation of the steady transfer films on the counterface during the repetitive sliding action. The friction coefficients of PTFE and PTFE-1 decrease a little with increase in the friction time. The friction coefficients of other nanocomposites, however, have the opposite tendency. Changes in the friction coefficients for PTFE-2 and PTFE-3 are between ~0.18 and 0.19, a small improvement

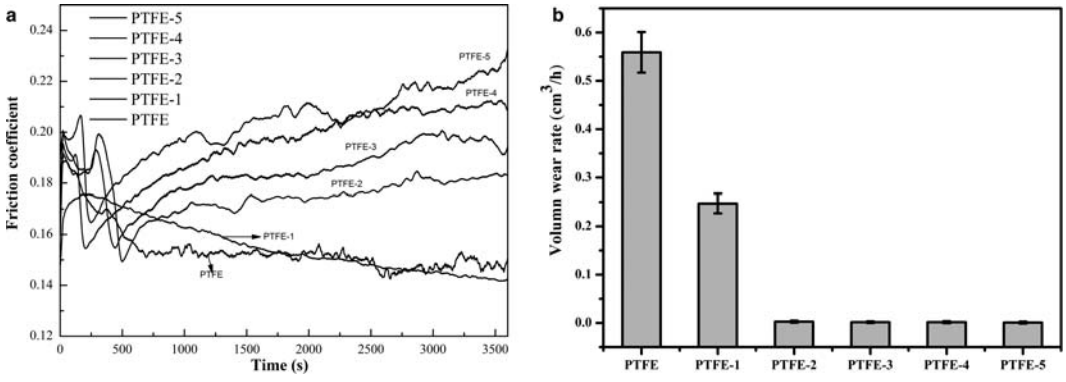

FIG. 7. Friction coefficients and volume wear rates of PTFE and PTFE nanocomposites: (a) PTFE; (b) PTFE-1; (c) PTFE-2; (d) PTFE-3; (e) PTFE-4; and (f): PTFE-5.

https://doi.org/10.1180/claymin.2017.052.4.02 Published online by Cambridge University Press

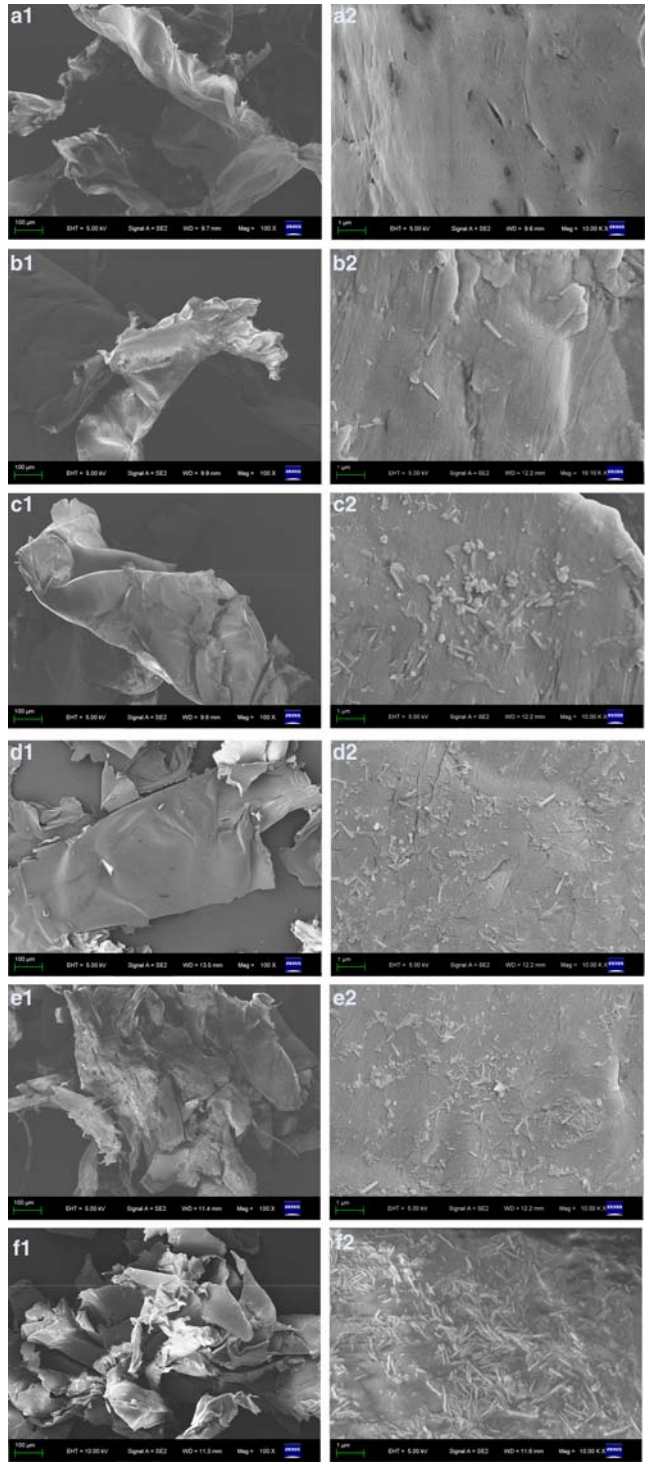

FIG. 8. SEM images of the wear debris of PTFE and PTFE nanocomposites: (a) PTFE; (b) PTFE-1; (c) PTFE-2; (d) PTFE-3; (e) PTFE-4; and (f) PTFE-5.

https://doi.org/10.1180/claymin.2017.052.4.02 Published online by Cambridge University Press

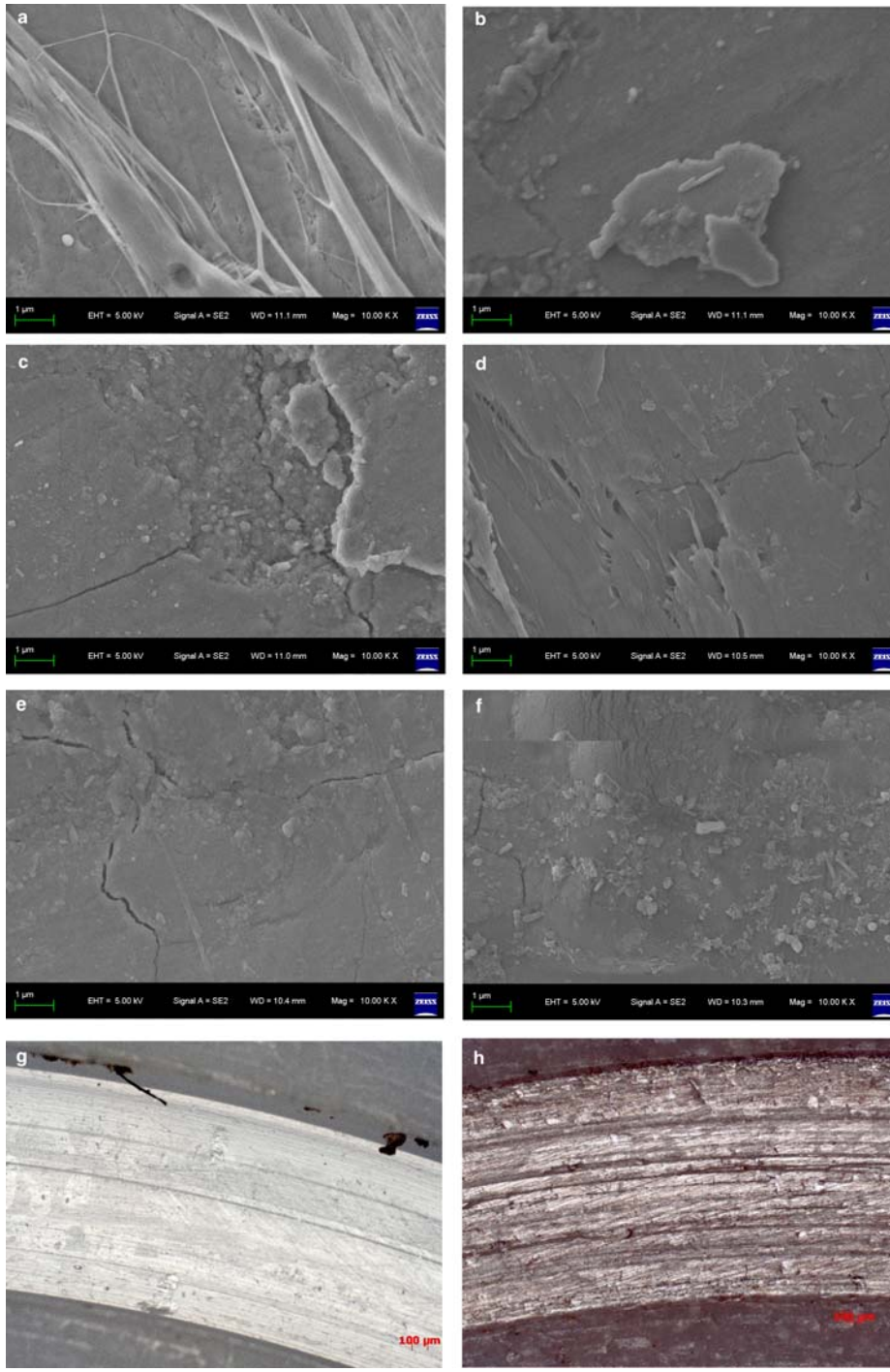

FIG. 9. SEM (a–f) and 3D laser scanning microscope (g,h) images of the worn surface of PTFE and HNT/PTFE nanocomposites: (a,g) PTFE; (b) PTFE-1; (c,h) PTFE-2; (d) PTFE-3; (e) PTFE-4; and (f) PTFE-5.

https://doi.org/10.1180/claymin.2017.052.4.02 Published online by Cambridge University Press

compared to PTFE. However, the friction coefficients of PTFE-4 and PTFE-5 increased from 0.18 at the beginning to 0.23 at the end. The addition of larger amounts of HNTs to PTFE results, therefore, in a distinct increase in the friction coefficient, which is attributed to the poor dispersion of HNTs at high filling contents in the PTFE matrix. It may be that the transfer film formed on a counterface during sliding plays an important role in the tribological behaviour of polymers. The enrichment of HNTs in the transfer film leads to the obvious improvement in the friction coefficient.

Figure 7b shows the volume wear rate of pure PTFE and of PTFE nanocomposites. The testing of the nanocomposites ensured a steady-state wear rate, which can be quantified. The results show that the incorporation of HNTs could cause a dramatic improvement in the wear behaviour of PTFE. Compared to unfilled PTFE, the volume wear rate of the HNTs/PTFE nanocomposites at 2 wt.% HNTs is 21 times less than that of pure PTFE; meanwhile the tensile strength increased by 3.5%. To the present authors' knowledge, a crystal of PTFE has a ribbon-like structure and a smooth surface and consists of macromolecular chains. A single crystal is hexagonal and 20–50 nm thick. Because the outer diameter of HNTs is ~40 nm, *i.e.* of the same order of magnitude as the dimensions of single crystals of PTFE, HNTs can intertwine with crystals of PTFE. Because of their stronger mechanical properties and greater aspect ratio, HNTs are able to reinforce PTFE composites significantly, and thus to prevent the crystal structure of PTFE from being destroyed during the friction test. Although crystals of PTFE are drawn out from a PTFE surface by shear during a friction test, HNTs impede this drawing-out of PTFE crystals effectively, and thus improve the wear resistance of HNTs/PTFE composites significantly. Furthermore, the presence of HNTs in the friction interface act as effective barriers to prevent large-scale fragmentation of PTFE and slow the formation of a transfer film. When sliding against the steel counterpart, the load can be transferred to the HNTs, the wear resistance of which is much greater than that of pure PTFE.

Figure 8 shows the wear debris for pure PTFE and HNTs/PTFE nanocomposites. In Fig. 8a1–f1 the wear debris fragments produced by the friction process are smaller for the pure PTFE than for the nancomposites. It is likely that the smaller wear debris remains at the contact for longer during the friction process. Some smaller debris particles and HNTs could even remain in 'roughness valleys' throughout the entire process (Wang & Yan, 2006).

From Fig. 8a2–f2 the debris surface of pure PTFE with some gaps looks smoother (Fig. 8a2). With the addition of small amounts of HNTs (2 wt.%), the wear debris of the nanocomposite is more like that of pure PTFE except for some where there is dispersion of the HNTs. Thus, the amount of debris increases with increase in the amount of HNTs. During the sliding process, the wear debris which is smooth and large is extruded more easily from the contact region and this explains the poor wear behaviour of pure PTFE. With the addition of HNTs, the wear debris is rougher and smaller than that of pure PTFE. This phenomenon may slow the formation of transfer film and improve the wear behaviour of the nanocomposites.

Figure 9 shows the worn surface of pure PTFE and HNTs/PTFE nanocomposites. As for pure PTFE, the obvious banding tears can be distinguished due to the sliding behaviour between polymer and steel. This phenomenon proves the poor wear resistance of PTFE because of the weak Van der Waals forces between the PTFE modules (Lee *et al*., 2007; Krick *et al*., 2015). As shown in Fig. 9b–d, corresponding to proportions of 2, 5 and 10 wt.% of HNTs, subsurface damage and material loss have occurred due to the repeated sliding. The particles broken and released from the composites have initiated the debonding and then the elongated cracks, and subsequently led to large amounts of debris which resulted in a significant abrading wear rate. At 15 and 20 wt.% of HNTs (Fig. 9e,f), there are no large banding tears or serious damage to the worn surfaces. This is consistent with the better wear behaviour of the HNTs/PTFE nanocomposites than that of pure PTFE. Note that a number of HNTs appear on the worn surface. This is due to the super-strong mechanical properties and the high aspect ratio of HNTs; the HNTs in the worn surface protect the PTFE from serious damage. Figure 9g,h shows the 3D laser scanning microscopy image of pure PTFE and PTFE-2. As for pure PTFE, the surface is smooth. The microgrooves and banding tears can be seen clearly in the worn surface. The reason is that the Van der Waals forces of the PTFE molecules are weak. This phenomenon confirms the poor wear behaviour of pure PTFE. In Fig. 9h, the worn surface is rugged, which is because the incorporation of HNTs shares the load with PTFE resin and HNTs exist between the counterpart and PTFE resin to decrease the wear rate.

CONCLUSIONS

Using halloysite nanotubes (HNTs) as reinforcing fillers, and a cold compression moulding method, HNTs/PTFE

https://doi.org/10.1180/claymin.2017.052.4.02 Published online by Cambridge University Press

nanocomposites with significant wear resistance were prepared. The effect of HNTs in PTFE in terms of structure and performance were investigated comprehensively. At an optimal filling amount of 2 wt.%, the wear rate of the nanocomposites reduced by ∼90% compared to pure PTFE while the tensile strength was increased by ∼3.5%. To further improve the mechanical and wear resistance of HNTs/PTFE nanocomposites, modification of the HNTs to promote the dispersion and solve the interfacial issue in the PTFE polymer will enhance the properties of the polymer nanocomposites. HNTs are therefore an excellent and low-cost reinforcing filler for high-performance polymers

ACKNOWLEDGEMENTS

This work was funded by the Talent Introduction Fund of Yangzhou University (2012), Zhenjiang High Technology Research Institute of Yangzhou University (2017), Key Research Project-Industry Foresight and General Key Technology of Yangzhou (YZ2015020), Innovative Talent Program of Green Yang Golden Phoenix (yzlyjfjh2015CX073), Yangzhou Social Development Project (YZ2016072), Jiangsu Province Six Talent Peaks Project (2014-XCL-013) and Jiangsu Industrial-academic-research Prospective Joint Project (BY2016069-02). The authors also acknowledge the project funded by the Priority Academic Program Development of Jiangsu Higher Education Institutions and Top-notch Academic Programs Project of Jiangsu Higher Education Institutions (PPZY2015B112). The data published here originated from the Test Center of Yangzhou University.

REFERENCES

Ahmadi S.J., Huang Y.D. & Li W. (2005) Fabrication and physical properties of EPDM-organoclay nanocomposites. *Composites Science and Technology*, **65**, 1069–1076.

Carli L.N., Daitx T.S., Soares G.V., Crespo J.S. & Mauler R.S. (2014) The effects of silane coupling agents on the properties of PHBV/halloysite nanocomposites. *Applied Clay Science*, **87**, 311–319.

Čermák M., Kadlec P., Šutta P. & Polanský R. (2016) Structural and mechanical behaviour of LLDPE/HNT nanocomposite films. *International Conference of Polymer Processing Society*, **17**, 574–582.

Chen W.X., Li F., Han G., Xia J.B., Wang L.Y., Tu J.P. & Xu Z.D. (2003) Tribological behavior of carbon-nanotube-filled PTFE composites. *Tribology Letters*, **215**, 275–278.

Cheng Z.L. & Sun W. (2016) Structure and physical properties of halloysite nanotubes. *Acta Petrolei Sinica (Petroleum Processing Section)*, **32**, 123–128.

Dong Y., Marshall J., Haroosh H.J., Mohammadzadehmoghadam S., Liu D.Y., Qi X.W. & Lau K.T. (2015) Polylactic acid (PLA)/halloysite nanotube (HNT) composite mats: influence of HNT content and modification. *Composites Part A, Applied Science & Manufacturing*, **76**, 28–36.

Du M.L., Guo B.C. & Jia D.M. (2006) Thermal stability and flame retardant effects of halloysite nanotubes on poly (propylene). *European Polymer Journal*, **42**, 1361–1369.

Handge U.A., Hedicke-Höchstötter K. & Altstädt V. (2010) Composites of polyamide 6 and silicate nanotubes of the mineral halloysite: influence of molecular weight on thermal, mechanical and rheological properties. *Polymer*, **51**, 2690–2699.

Ismail H., Pasbakhsh P., Ahmad Fauzi M.N. & Bakar A.A. (2008) Morphological, thermal and tensile properties of halloysite nanotubes filled ethylene propylene diene monomer (EPDM) nanocomposites. *Polymer Testing*, **27**, 841–850.

Jia Z.X., Luo Y.F., Guo B.C., Yang B.T., Du M.L. & Jia D.M. (2009) Reinforcing and flame-retardant effects of halloysite nanotubes on LLDPE. *Polymer-Plastics Technology and Engineering*, **48**, 607–613.

Klaas N.V., Marcus K. & Kellock C. (2005) The tribological behaviour of glass filled polytetrafluoroethylene. *Tribology International*, **38**, 824–833.

Krick B.A., Pitenis A.A., Harris K.L., Junk C.P., Sawyer W.G., Brown S.C., Rosenfeld H.D., Kasprzak D.J., Johnson R.S., Chan C.D. *et al.* (2015) Ultralow wear fluoropolymer composites: nanoscale functionality from microscale fillers. *Tribology International*, **95**, 245–255.

Kwong H.Y., Wong M.H., Wong Y.W. & Wong K.H. (2006) Magnetoresistivity of cobalt-polytetrafluoroethylene granular composites. *Applied Physics Letters*, **89**, 173109.

Lee J.Y., Lim D.P. & Lim D.S. (2007) Tribological behavior of PTFE nanocomposite films reinforced with carbon nanoparticles. *Composites: Part B*, **38**, 810–816.

Leszczyńska A., Njuguna J., Pielichowski K. & Banerjee J.R. (2007) Polymer/montmorillonite nanocomposites with improved thermal properties: Part II. Thermal stability of montmorillonite nanocomposites based on different polymeric matrixes. *Thermochimica Acta*, **454**, 1–22.

Lim S.T., Yang H.H., Choi H.J. & Jhon M.S. (2002) Synthetic biodegradable aliphatic polyester/montmorillonite nanocomposites. *Chemistry of Materials*, **14**, 1839–1844.

Liu M.X., Guo B.C., Du M.L. & Jia D.M. (2007a) Drying induced aggregation of halloysite nanotubes in polyvinyl alcohol/halloysite nanotubes solution and its effect on properties of composite film. *Applied Physics A*, **88**, 391–395.

Liu M.X., Guo B.C., Du M.L. & Jia D.M. (2007b) Properties of halloysite nanotube epoxy resin hybrids and the interfacial reactions in the systems.

https://doi.org/10.1180/claymin.2017.052.4.02 Published online by Cambridge University Press

Nanotechnology, **18**, 455703. DOI:10.1088/0957-4484/18/45/455703.

Liu P., Lu R.G., Huang T., Wang H.Y. & Li T.S. (2012) A study on the mechanical and tribological properties of carbon fabric/PTFE composites. *Journal of Macromolecular Science Part B*, **85**, 786–797.

Liu M.X., Zhang Y. & Zhou C.R. (2013a) Nanocomposites of halloysite and polylactide. *Applied Clay Science*, **75-76**, 52–57.

Liu M.X., Wu C.C., Jiao Y.P., Xiong S. & Zhou C.R. (2013b) Chitosan–halloysite nanotubes nanocomposite scaffolds for tissue engineering. *Journal of Materials Chemistry B*, **1**, 2078–2089.

Liu Y., Qiang C., Li H. & Zhang J. (2013c) Fabrication and characterization of mesoporous carbon nanosheets using halloysite nanotubes and polypyrrole via a template-like method. *Journal of Applied Polymer Science*, **128**, 517–522.

Liu M.X., Jia Z.X., Jia D.M. & Zhou C.R. (2014) Recent advance in research on halloysite nanotubes-polymer nanocomposite. *Progress in Polymer Science*, **39**, 1498–1525.

Liu M.X., Chang Y.Z., Yang J., You Y.Y., He R., Chen T.F. & Zhou C.R. (2016a) Functionalized halloysite nanotube by chitosan grafting for drug delivery of curcumin to achieve enhanced anticancer efficacy. *Journal of Materials Chemistry B*, **4**, 2253–2263.

Liu M.X., He R., Yang J., Long Z., Huang B., Liu Y.W. & Zhou C. (2016b) Polysaccharide-halloysite nanotube composites for biomedical applications: a review. *Clay Minerals*, **51**, 457–467.

Liu Z., Li Y.X., Ma L., Qin D.Z. & Cheng Z.L. (2017) A study of tribological properties of polypropylene nanocomposites reinforced with pretreated HNTs. *China Petroleum Processing and Process Research*, **19**, 115–124.

Lvov Y. & Abdullayev E. (2013) Functional polymer–clay nanotube composites with sustained release of chemical agents. *Progress in Polymer Science*, **38**, 1690–1719.

McElwain S.E., Blanchet T.A., Schadler L.S. & Sawyer W.G. (2008) Effect of particle size on the wear resistance of alumina-filled PTFE micro- and nano-composites. *Tribology Transactions*, **51**, 247–253.

Pasbakhsh P., Ismail H., Ahmad Fauzi M.N. & Bakar A.A. (2009) The partial replacement of silica or calcium carbonate by halloysite nanotubes as fillers in ethylene propylene diene monomer composites. *Applied Polymer and Science*, **113**, 3910–3919.

Pasbakhsh P., Ismail H., Ahmad Fauzi M.N. & Bakar A.A. (2010) EPDM/modified halloysite nanocomposites. *Applied Clay Science*, **48**, 405–413.

Razi A.F., Atieh M.A., Girun N., Chuah T.G., EI-Sadig M. & Biak D.R.A. (2003) Effect of multi-wall carbon nanotubes on the mechanical properties of natural rubber. *Composite Structures*, **14**, 641–649.

Vail J.R., Burris D.L. & Sawyer W.G. (2009) Multifunctionality of single-walled carbon nanotube–polytetrafluoroethylene nanocomposites. *Wear*, **267**, 619–624.

Vohra K., Anand A., UI Haq M.I., Raina A. & Wani M.F. (2016) Tribological characterization of a self-lubricating PTFE under lubricated conditions. *Materials Focus*, **5**, 1–4.

Wang Y.X. & Yan F.Y. (2006) Tribological properties of transfer films of PTFE-based composites. *Wear*, **261**, 1359–1366.

Ye Y.P., Chen H.B., Wu J.S. & Chan C.M. (2011) Evaluation on the thermal and mechanical properties of HNT-toughened epoxy/carbon fibre composites. *Composites Part B Engineering*, **42**, 2145–2150.

https://doi.org/10.1180/claymin.2017.052.4.02 Published online by Cambridge University Press